

Figure S1. SEM images of the Ti glycolate prepared with (a) 6ml formic acid, (b-f) 0ml, 3ml, 6ml, 12ml and 24ml water in acetone bath, respectively.

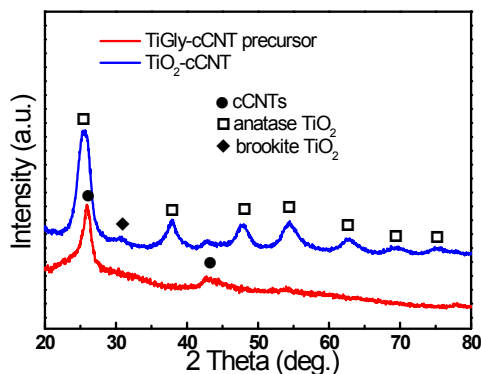


Figure S2. XRD spectra of the TiGly-cCNT precursor and its hydrolysis product. Clearly, after the hydrolytic decomposition in boiling water for 1h, the amorphous Ti glycolate is converted into anatase TiO_2 .

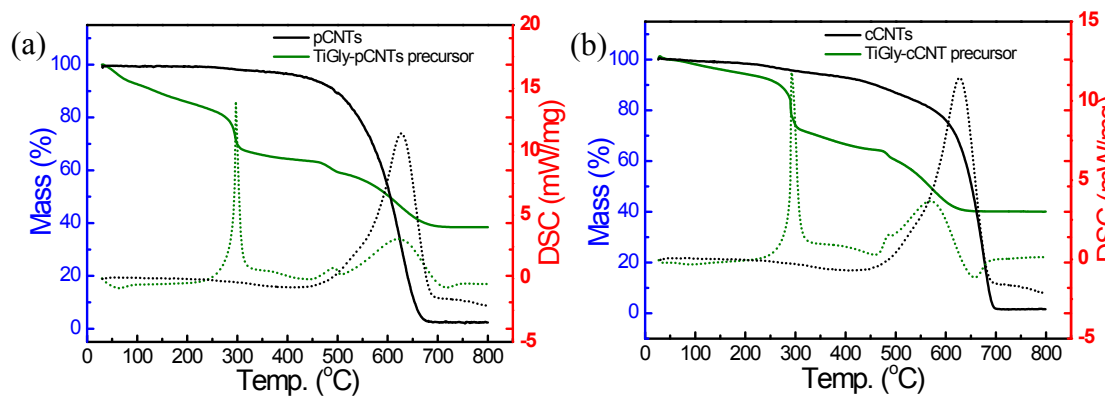


Figure S3. TG-DSC curves of (a) the pCNTs and TiGly-pCNT precursor and (b) the cCNTs and TiGly-cCNT precursor.

Synthesis and Results of the mSnO₂-cCNT and mCu₂O/CuO-cCNT

Synthesis of the mSnO₂-cCNT: 0.3 g stannous oxalate and 100 ml ethylene glycolate were refluxed at 85 °C for 24 h to prepare a Sn glycolate polymer solution. Then this polymer solution was poured to the acetone bath containing 170 mL acetone, 6 mL water and 0.1 g cCNTs for 1 h to prepare Sn glycolate coated-carboxylated CNT (denoted as SnGly-cCNT) precursor. The mSnO₂-cCNT was obtained by a pyrolytic decomposition of SnGly-cCNT precursor at 350 °C under air atmosphere for 2 h.

Synthesis of the mCu₂O/CuO-cCNT: 0.5 g copper acetate and 50 ml ethylene glycolate were refluxed at 85 °C for 1 h to prepare a Cu glycolate polymer solution. Then the Cu glycolate coated-carboxylated CNT (denoted as CuGly-cCNT) precursor was obtained after mixing this polymer solution to an acetone bath for 1 h. The acetone bath contained 170 ml acetone, 24 ml water and 0.05 g cCNTs. The mCu₂O/CuO-cCNT was obtained by a pyrolytic decomposition of CuGly-cCNT precursor at 300 °C under air atmosphere for 2 h.

The SnGly-cCNT and CuGly-cCNT precursors are firstly obtained respectively by the similar process of TiGly-cCNT. TG-DSC curves (Figure S4a, 4b) of these two precursors and XRD spectra (Figure S4c, 4d) of the pyrolysis decomposition products definitely demonstrate the conversion of Sn and Cu glycolates

into rutile SnO_2 and a mixture of Cu_2O with CuO , respectively. Note that the temperature shifts of cCNTs oxidation for SnGly-cCNT and CuGly-cCNT precursors are 62 °C and 130 °C, respectively. These remarkable reductions indirectly prove the uniformity of the two precursors.

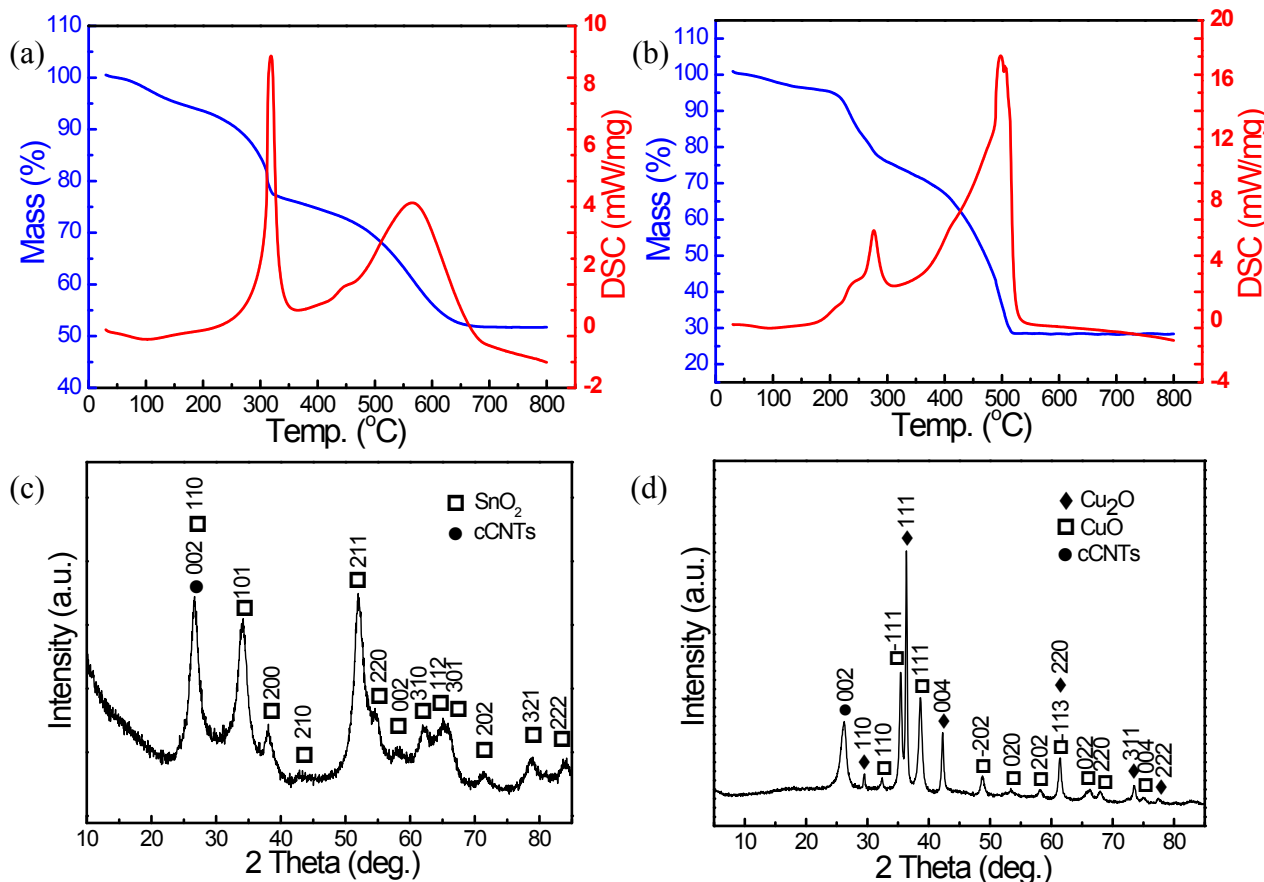


Figure S4. TG-DSC curves of (a) the SnGly-cCNT and (b) the CuGly-cCNT precursors. XRD spectra of (c) the m SnO_2 -cCNT and (d) the m $\text{Cu}_2\text{O}/\text{CuO}$ -cCNT.

Figure S5a is the SEM image of the SnGly-cCNT precursor. Similar with the morphology of the TiGly-cCNT, only 1-dimensional structures without Sn glycolate spheres are observed. The TEM and HRTEM images of the m SnO_2 -cCNT (Figure S5b, 5c) display that each cCNT is coated by a layer of interconnected SnO_2 nanoparticles. The size of the SnO_2 nanoparticles is smaller than 10 nm, and the thickness of the coating layer is about 7 nm. The morphology characterization of the CuGly-cCNT precursor and the m $\text{Cu}_2\text{O}/\text{CuO}$ -cCNT shown in Figure S5d-5f clearly indicate a thin deposition layer of $\text{Cu}_2\text{O}/\text{CuO}$

nanoparticles. The porous structure of the mSnO₂-cCNT and mCu₂O/CuO-cCNT are shown in Figure S5g, 5h, respectively. An enhancement of BJH pore size distribution in 2-7 nm after coating cCNTs with SnO₂ or Cu₂O/CuO also proves the mesoporous nature of the metal oxide coatings. Small clearances among nanocrystals of the coatings contribute to the increase of mesopores. The BET specific area of the mSnO₂-cCNT and mCu₂O/CuO-cCNT are 60.5 m²/g and 51.9 m²/g, respectively.

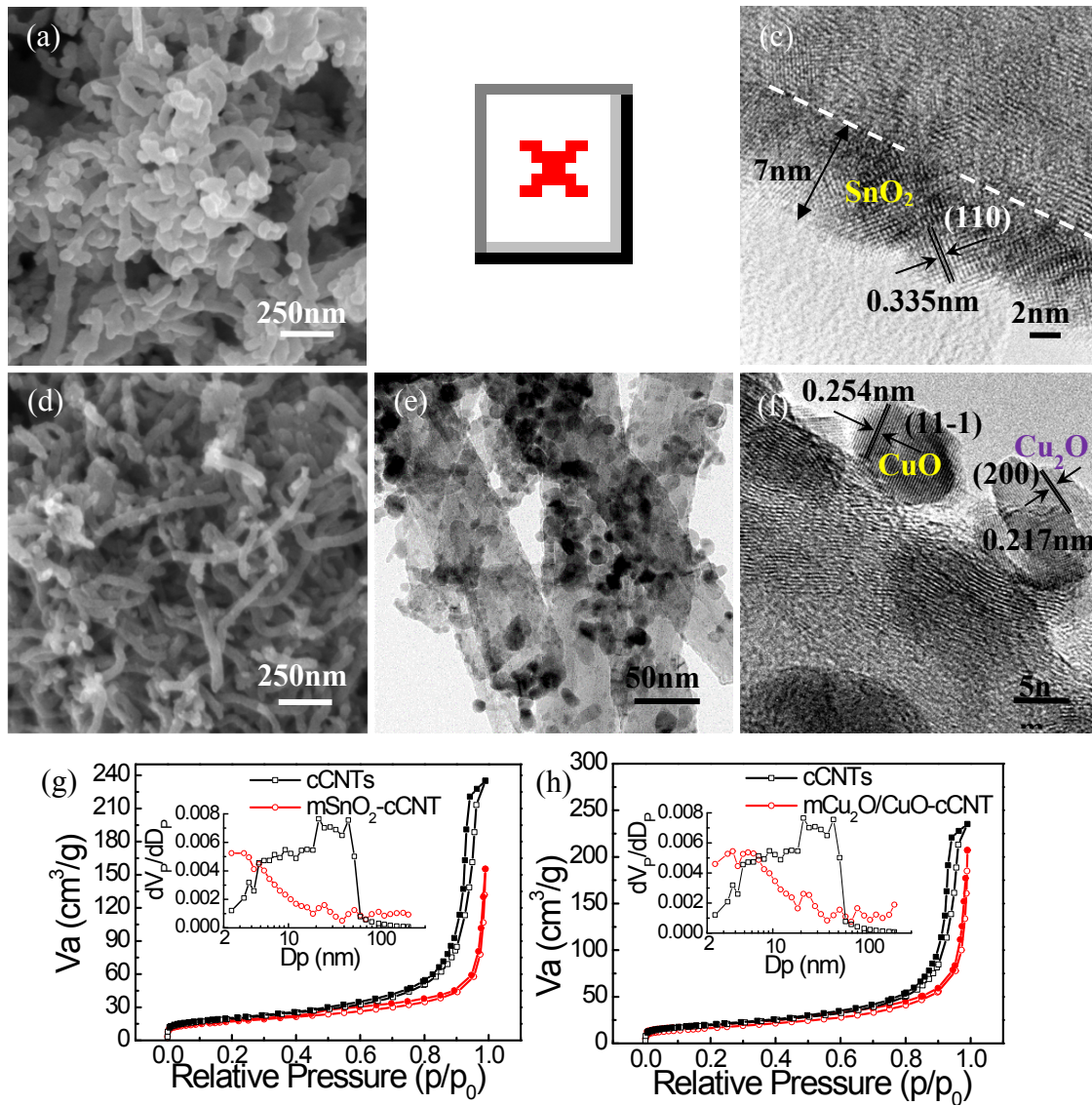


Figure S5. (a) SEM image of the SnGly-cCNT precursor. (b) TEM image and (c) HRTEM image of the mSnO₂-cCNT. (d) SEM image of the CuGly-cCNT precursor. (e) TEM image and (f) HRTEM image of the

mCu₂O/CuO-cCNT. N₂ adsorption-desorption curves and BJH pore size distribution curves (insert) of (g) the cCNTs and mSnO₂-cCNT and (h) the cCNTs and mCu₂O/CuO-cCNT.

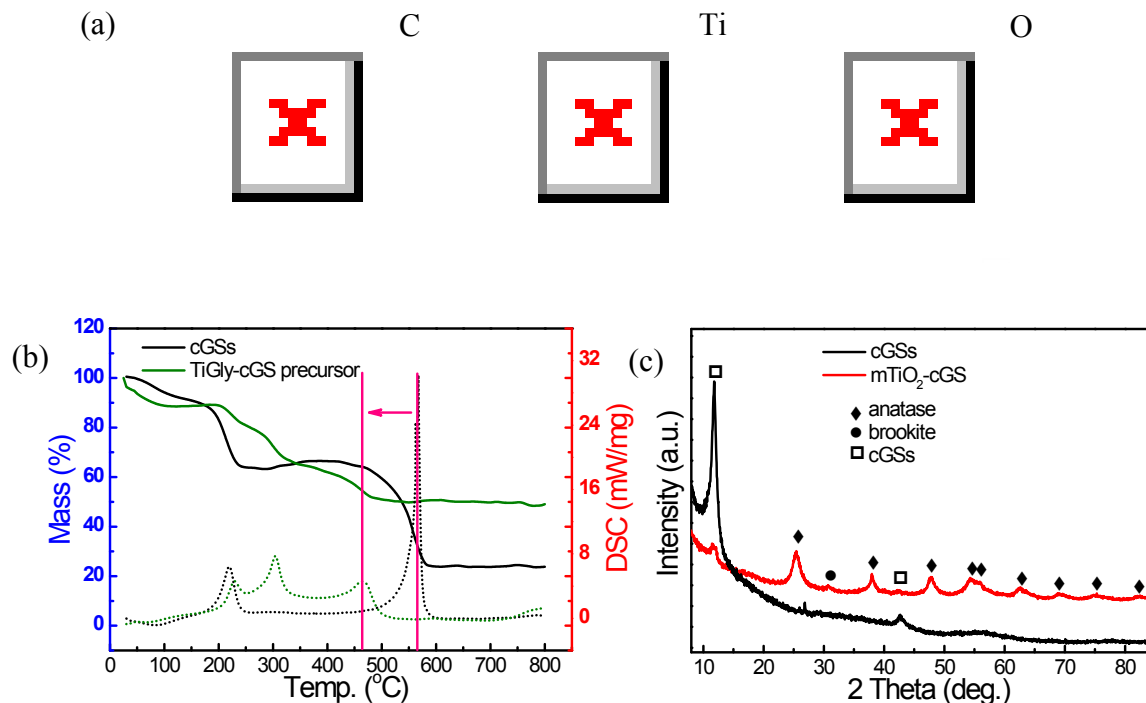


Figure S6. (a) Elemental mapping of the TiGly-cGS precursor. (b) TG-DSC curves of the cGSs and TiGly-cGS precursor. Clearly, the peak temperature of the exothermic oxidation of cGSs in TiGly-cGS precursor move ahead as much as 103 °C in comparison with that of the bare cGSs. This also indicates the uniformity of Ti glycolate on cGSs. (c) XRD spectra of the cGSs and mTiO₂-cGS. Major anatase TiO₂ and cGSs together with a little brookite TiO₂ are identified. The peak observed at $2\theta = 10.45^\circ$ is corresponding to an average interlayer spacing of ~ 0.78 nm for the cGSs.